



A thiophene-modified screen printed electrode for detection of dengue virus NS1 protein

M.M.S. Silva^a, A.C.M.S. Dias^a, M.T. Cordeiro^b, E. Marques Jr.^{b,c}, M.O.F. Goulart^d, R.F. Dutra^{a,*}

^a Biomedical Engineering Laboratory, Federal University of Pernambuco, Av. Prof. Moraes Rego, 1235, Cidade Universitária, 50670-901 Recife, Brazil

^b Aggeu Magalhães Research Center, FIOCRUZ-PE, Recife, Brazil

^c Center for Vaccine Research, University of Pittsburgh, Pittsburgh, PA, USA

^d Institute of Chemical and Biotechnology, Federal University of Alagoas, Maceió, Brazil

ARTICLE INFO

Article history:

Received 15 February 2014

Received in revised form

7 June 2014

Accepted 8 June 2014

Available online 14 June 2014

Keywords:

Screen printed electrode

Thiophene

Dengue virus

Immunosensor

ABSTRACT

A thiophene-modified screen printed electrode (SPE) for detection of the Dengue virus non-structural protein 1 (NS1), an important marker for acute phase diagnosis, is described. A sulfur-containing heterocyclic compound, the thiophene was incorporated to a carbon ink to prepare reproducible screen printed electrodes. After cured, the thiophene SPE was coated by gold nanoparticles conjugated to Protein A to form a nanostructured surface. The Anti-NS1 antibodies immobilized via their Fc portions via Protein A, leaving their antigen specific sites free circumventing the problem of a random antibodies immobilization. Amperometric responses to the NS1 protein of dengue virus were obtained by cyclic voltammetries performed in presence of ferrocyanide/ferricyanide as redox probe. The calibration curve of immunosensor showed a linear response from $0.04 \mu\text{g mL}^{-1}$ to $0.6 \mu\text{g mL}^{-1}$ of NS1 with a good linear correlation ($r=0.991$, $p < 0.05$). The detection limit ($0.015 \mu\text{g mL}^{-1}$ NS1) was lower than conventional analytical methods. In this work, thiophene monomers incorporated in the carbon ink enhanced the electroanalytical properties of the SPEs, increasing their reproducibility and sensitivity. This point-of-care testing represents a great potential for use in epidemic situations, facilitating the early diagnosis in acute phase of dengue virus.

© 2014 Elsevier B.V. All rights reserved.

1. Introduction

Dengue is a significant public health threat, with estimates of 50 to 100 million cases per year and around 3 billion people at risk of infection, mainly in tropical and subtropical regions [1]. Infection can result in a broad spectrum of disease syndromes ranging from an asymptomatic or mild infection, classical dengue fever (DF), to the potentially fatal dengue haemorrhagic fever (DHF) and dengue shock syndrome [2]. So far, there is no effective anti-viral therapeutic on the market and supportive therapy such as fluid replacement is the only treatment for severe forms of the disease. An early and accurate laboratory diagnosis of dengue could assist clinical management [3]. An ideal blood test for diagnostic should be affordable and easy to use with high performance and sensitivity to distinguish the acute-phase of dengue [4]. Additionally, it should not be costly and not require several steps, being adaptable at laboratory or at a point-of-care diagnostic without compromising its accuracy [5].

The most important development in dengue diagnostics in recent years is the advent of the specific detection of dengue virus NS1 antigen [6]. Enzyme-linked immunosorbent assays (ELISA) for detecting the NS1 were developed and demonstrated excellent sensitivity and specificity in detection of dengue infections [6–8]. NS1 glycoprotein is circulating mostly from days 1–6 after the onset of clinical symptoms, with the peak NS1 antigen detection occurring between days 3 and 5, in both primary and secondary infections, and hence is an excellent diagnostic target for acute dengue diagnosis [4,8]. Although the classical techniques are very powerful for monitoring, they are time consuming and are not adaptable for in situ and real time detection, beyond require skilled personnel [9,10]. Alternatively, rapid diagnostic test (RDT) for NS1 detection based on immunochromatography was proposed [11]. However, even if RDTs can provide opportunities for point-of-care, they have limitations regarding detectability, once their results are limited to a qualitative analyses (yes/no), becoming difficult the diagnostic of the acute-phase of dengue that is correlated with NS1 levels. Contrary, biosensors can supplier quantitative responses through a transducer that converts biochemical reactions in a measurable electric signal [12].

Electrochemical biosensors employing screen printed electrodes have emerged as adequate tools for point-of-care testings. They have

* Corresponding author. Tel.: +55 81 21268200.

E-mail address: rosa.dutra@ufpe.br (R.F. Dutra).

innumerable advantages, such as ease of mass production and versatility [13]. Screen printed electrodes (SPEs) can combine good electrochemical properties and portability with simple and inexpensive fabrication techniques, thus being a good strategy to accomplish safety, disposable and quantitative immunosensors [14]. In the fabrication of SPEs are used inks containing different chemical compounds, polymers or functional linking that can be printed onto diverse type of plastic or ceramic substrates. The incorporation of compounds in the inks used for printing on the electrodes is a determinant factor for their selectivity and sensitivity required for each analysis [15].

Thiophene monomer derivatives have been pointed as attractive compounds to prepare electrochemical sensor, because they increase the conductivity, reduce the redox potential and improve the thermal and electrochemical stability [16]. Herein, thiophene monomers were incorporated into the carbon ink to form a homogenous and conductive composite, supplying a suitable signal amplification strategy to improve the electrochemical characteristics of the SPE increasing the sensitivity due to higher current densities and charge transfer across the interface electrode–electrolyte. Furthermore, sensitivity of immunosensors can be improved by increasing the amount of antibody immobilized on the electrode surface. Variety of nanostructures materials, with similar dimensions to biomolecules (antibodies, enzymes, DNA) owning different sizes, shapes and exceptional properties; such as metal nanoparticles (NP), quantum dots, carbon nanotubes and nanowires have employed for improvement of electrochemical biosensors. Nevertheless, NP which has capability for in situ synthesis onto the various composite films for antibody immobilization can improve the electrochemical signal and adsorption capacity of antibodies, and consequently enhance detection sensitivity. Therefore, the use of NPs represents a promising integration of electrochemical methods with new nanomaterials and electroactive complexes for electrochemical immunosensing [17].

It is well-known that way as antibodies are immobilized on the electrode surface affects the performance of an immunosensor. Fab portions of antibodies should be free for recognizing and binding to the epitopes of antigens. The Protein A extracted from *Staphylococcus aureus* has high affinity to the Fc portion of immunoglobulins from a variety of species, being widely used to promote an oriented antibody immobilization [18]. When the Protein A was used in a chromatographic assay, it was capable of binding antigen at over 80% of their theoretical capacity, because of the increased strength of the couple between the antibody Fc portion and protein A [19]. Stable and oriented immobilization of antibodies combined with the electrochemical advantages of thiophene as chemical modifying compound allowed an accurate detection of NS1. No labels were necessary when the antigen–antibody interactions were registered. The method described herein involves one-step preparation process and represents an advance in the production of SPEs for point-of-care testing.

2. Experimental

2.1. Materials and reagents

2.1.1. Chemical reagents and materials

Electrode PF-407 C carbon ink with a density of 1.13 kg cm^{-3} was acquired from Acheson Henkel Corporation (Port Huron, MI, USA). Thiophene, protein A–conjugated gold nanoparticles (PtnA–AuNP) with approximately 20 nm (P6855), potassium ferricyanide ($\text{K}_3[\text{Fe}(\text{CN})_6]$), potassium ferrocyanide ($\text{K}_4[\text{Fe}(\text{CN})_6]$) and glycine, were acquired from Sigma–Aldrich (St. Louis, MO, USA). Phosphate buffer saline (PBS) (10 mmol L^{-1} , pH 7.4) used in all experiments was prepared by dissolving 0.2 g KCl, 8.0 g NaCl, 0.24 g KH_2PO_4

and 1.44 g Na_2HPO_4 , in 1000 mL of deionized Milli-Q water from Millipore units (Bedford, MA, USA). All chemicals were of analytical grade.

2.1.2. Biological reagents

Mouse monoclonal antibodies against the NS1 glycoprotein of dengue virus (ab 138696) used to electrodes preparation and the dengue virus NS1 recombinant full-length protein (ab 64456) were purchased from Abcam (Cambridge, MA, USA). NS1 native protein was obtained from DENV-3 (strain 101.905/BR-PE/03) culture supernatant collected on the 5th day after inoculation in C6/36 cell monolayers, maintained in Leibovitz L-15 medium (GIBCO, Invitrogen, Grand Island, NY) containing 2% fetal calf serum. DENV-3 was detected and identified by RT-PCR [20]. In house ELISA, using anti-NS1 monoclonal antibodies, confirmed the presence of NS1 native protein in virus culture supernatant. As control was used supernatant from C6/36 cell culture (without virus) collected in the same conditions. Both supernatants were cleared by centrifugation for 10 min at 1500 rpm (400 g).

2.2. Preparation of the thiophene-SPE

The electrodes were manufactured by squeezing a mixture containing carbon ink and thiophene onto a polyethylene terephthalate support to form a thin conductive film. Four different concentrations of thiophene in relation to carbon ink were tested: 0.5% (w/V); 1% (w/V); 2.5% (w/V) and 10% (w/V). Prior printing, a plastic mold was used onto the PET rectangular surface ($0.4 \times 1.0 \text{ cm}$) to ensure electrodes with equal areas. After manufacturing, the electrodes were cured at 60°C for 20 min. The manufactured thiophene-SPE consisted of with a circular area ($\varnothing=4 \text{ mm}$) joined to a rectangular area ($1 \text{ mm} \times 15 \text{ mm}$) used to electrical contact. After ready, the area of the electrode was delimited using a tape for galvanoplasty.

Prior to use, the thiophene-SPEs were pretreated by cyclic voltammetry (CV), scanning 30 cycles with a potential ranging from -2.0 V to 2.0 V , at a scan rate of 0.1 V s^{-1} and step potential of 2.44 mV, using 0.1 mol L^{-1} of KCl solution as the supporting electrolyte [21].

2.3. Apparatus

All the electrochemical experiments were performed in an Ivium Compact Stat potentiostat/galvanostat from Ivium Technologies (Eindhoven, The Netherlands) interfaced with a microcomputer and controlled by Ivium Soft software. A three-electrode system was used, which consisted of a thiophene-SPE as the working electrode (4 mm diameter), an Ag/AgCl electrode as the reference electrode and a helical platinum wire as the counter electrode. The electrodes were set up in a glassy electrochemical cell with 5 mL volume.

Experiments for characterizing the assembling of the thiophene-SPE were performed by CV in presence of 5 mmol L^{-1} of $\text{K}_3\text{Fe}(\text{CN})_6/\text{K}_4\text{Fe}(\text{CN})_6$ prepared in 0.1 mol L^{-1} of KCl solution, with a potential ranging from -0.6 V to 1.0 V , at 50 mV s^{-1} scan rate. Antigen–antibody interactions at the interface of the thiophene-SPE were also monitored by differential pulse voltammetry (DPV). DPV measurements were recorded from 0 V to 0.8 V, with pulse amplitude of 0.025 V, width of 0.05 s, and step potential of 0.05 V. The current signals were registered at a fixed potential (0.25 V) and the analytical response to NS1 was obtained taking into account the difference between the peak current (ΔI) of the thiophene-SPE with NS1 and the blank.

Fourier transform infrared (FTIR) spectra of samples were recorded by using a Bruker IFS 66 model FTIR spectrometer in

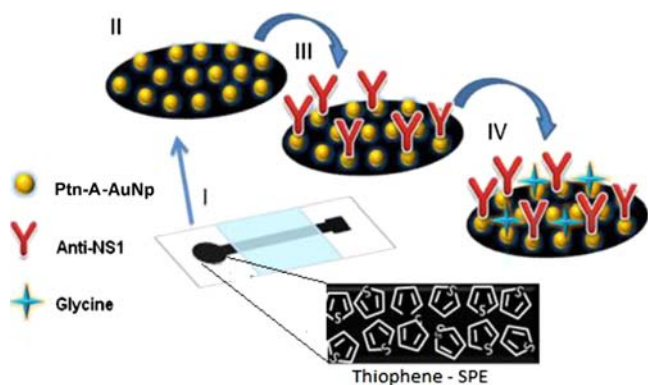


Fig. 1. Schematic illustration of the stepwise preparation of the NS1 immunosensor (I) bare thiophene-SPE; (II) AuNP-Ptn-A/thiophene-SPE; (III) anti-NS1/AuNP-Ptn-A/thiophene-SPE; and (IV) glycine/anti-NS1/AuNP-Ptn-A/thiophene-SPE.

the region of 4000 cm^{-1} to 400 cm^{-1} , by using the standard KBr pellet technique.

2.4. Immobilization of the anti-NS1

Anti-NS1 antibodies were immobilized via protein A-conjugated gold nanoparticle (AuNP-Ptn A), forming a nanostructured film on the electrode surface. $10\text{ }\mu\text{L}$ AuNP-Ptn A solution was pipetted onto the electrode surface of the thiophene-SPEs and left at $4\text{ }^\circ\text{C}$ (overnight). Subsequently, $10\text{ }\mu\text{L}$ of anti-NS1 ($10\text{ }\mu\text{g mL}^{-1}$) prepared in 10 mmol L^{-1} of PBS was incubated on the electrode surface for 1 h. Non-specific bindings were blocked by incubating the electrode surface with 50 mmol L^{-1} of glycine solution for 40 min. For preservation of the anti-NS1, the immobilized thiophene-SPE was stored in a moist chamber in a refrigerator (approximately $+4\text{ }^\circ\text{C}$). A schematic design of the thiophene-SPE is shown in Fig. 1.

2.5. Immunosensor response to NS1

Initially, the analytical responses of the immunosensor were evaluated by incubating the coated anti-NS1 thiophene-SPEs with NS1 samples in different concentrations. Then, $10\text{ }\mu\text{L}$ of NS1 solutions were pipetted on the electrode surface and left to react for 30 min in a moist chamber at room temperature ($24\text{ }^\circ\text{C}$). Afterwards, the electrode was washed four times in PBS and water. The immunosensor response was also evaluated in real samples against the NS1 native protein by incubating the anti-NS1 thiophene-SPEs with culture supernatant collected on the 5th day after inoculation in C6/36 cell monolayers. The supernatant solution containing NS1 native antigen was 1:128, 1:64, 1:32, 1:16, 1:8, 1:4 and 1:1 serial diluted in PBS and $10\text{ }\mu\text{L}$ of supernatant was also pipetted on the electrode surface at the same conditions described. A culture supernatant of C6/36 cells monolayers without NS1 infected serum inoculation was used as control.

3. Results and discussion

3.1. Characterization of thiophene-SPE

Chemically modified screen-printed carbon electrodes may be produced by incorporating specific reagents into the screen-printing inks, thus increasing the selectivity and detectability of measurements [22]. Among the available electroanalytical techniques, the CV technique has been widely used to understand the electroactivity and the electrochemical properties of conductor films or organic salts because it can better describe the

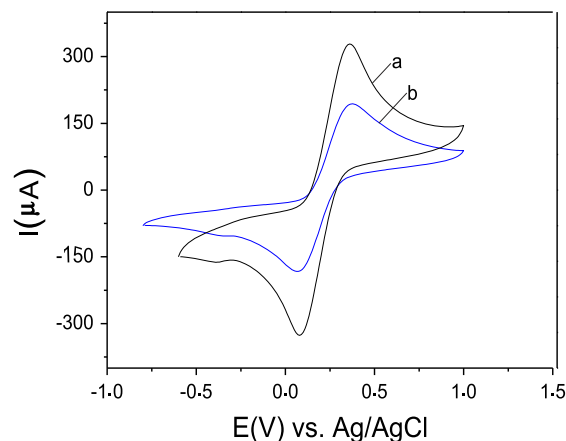


Fig. 2. (a) Cyclic voltammogram profiles of the carbon ink-printed electrode, with thiophene; and (b) without thiophene. The scans were performed in 5 mmol L^{-1} $\text{K}_3\text{Fe}(\text{CN})_6/\text{K}_4\text{Fe}(\text{CN})_6$, at a scanning rate of 50 mV s^{-1} .

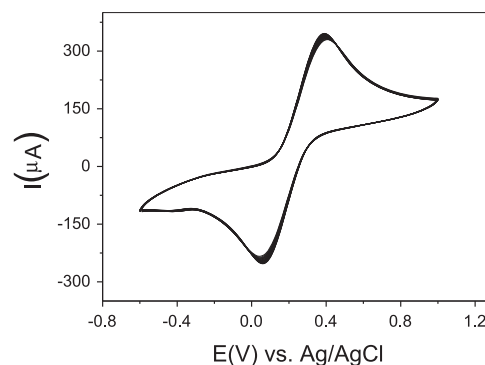


Fig. 3. Cyclic voltammograms of the thiophene-SPE from twenty replicate cycles performed in presence of 5 mmol L^{-1} of $\text{K}_3\text{Fe}(\text{CN})_6/\text{K}_4\text{Fe}(\text{CN})_6$ prepared in a 0.1 mol L^{-1} KCl solution, at a scanning rate of 50 mV s^{-1} .

characteristics of the electrochemical switching behavior between conducting and insulating states. Herein, the thiophene-SPE and the chemically-unmodified screen-printed carbon electrode were submitted to a CV technique in the presence of 5 mmol L^{-1} of $\text{K}_3\text{Fe}(\text{CN})_6/\text{K}_4\text{Fe}(\text{CN})_6$ prepared in 0.1 mol L^{-1} of KCl solution, at a 0.1 V s^{-1} scan rate and potential ranging from -0.6 V to 1.0 V (Fig. 2). The incorporation of the thiophene into the carbon ink resulted in an increase of approximately 40% of the current density. This behavior tells that the thiophene makes considerable contribution to higher charge transfer, improving the technical performance of carbon ink electrode.

The stability of the thiophene-SPE was also evaluated by setting the chemically-modified electrode to successive CVs. After 20 cycles performed in presence of 5 mmol L^{-1} of $\text{K}_3\text{Fe}(\text{CN})_6/\text{K}_4\text{Fe}(\text{CN})_6$ prepared in a 0.1 mol L^{-1} KCl electrolyte, at 0.1 V s^{-1} scanning rate and a potential ranging from -0.6 V to 1.0 V , the redox peaks were practically constant. It was obtained a coefficient of variation of approximately 3.4% that is much more stable than the electrode without thiophene (9.2% coefficient of variation) (Fig. 3).

3.2. Effect of thiophene concentration

The influence of thiophene concentration on the electrode performance were performed by using CV in presence of $\text{K}_3\text{Fe}(\text{CN})_6/\text{K}_4\text{Fe}(\text{CN})_6$ as redox probe. The concentrations of thiophene varied from 0.5% to 10%, were analyzed according to maximal amplitude of the produced redox peaks. It was found that the redox peaks increased with the thiophene concentration, achieving

a plateau at 2.5% (m/v) thiophene. The use of 2.5% of thiophene resulted conductivities two times greater than for non-modified electrodes (Fig. 4). Thus, this concentration was used in all remaining experiments.

3.3. Fourier transform infra-red (FTIR) spectroscopy

FTIR spectra were used to investigate the modification of the carbon ink with thiophene. The FTIR spectra of the carbon ink layer without thiophene are shown in Fig. 5. Typical spectra for several concentrations of carbon black (ink component) are shown in Fig. 5(a). A band at 1634 cm^{-1} is probably a high conjugated C=O. O'Reilly and Mosher [23] discuss the assignment of the 1600 cm^{-1} band in carbon black and they attributed to aromatic ring stretching frequencies whose intensity is enhanced by the presence of oxygen atoms as phenol or ether groups. Two peaks are required in the 1400 cm^{-1} to 1200 cm^{-1} region to reproduce the experimental curve. A band at 1400 cm^{-1} to 1450 cm^{-1} is assumed to be the C–O stretching frequency of the carboxylic acid group and a band at 1120 cm^{-1} to 1190 cm^{-1} , probably due to the coupled C–O stretching frequency and OH bending modes of COOH and possibly the C–O stretching modes of ethers.

After the incorporation of thiophene in the carbon ink, the spectral analysis showed functional groups of the thiophene (Fig. 5(b)). Two bands at 2920 cm^{-1} and 2850 cm^{-1} corresponding to the C–H stretching; at cm^{-1} to the C=C stretching, at 1250 cm^{-1} to the CH₂ stretching, at 1116 cm^{-1} to the bending vibrating peak of C–H, and 572 cm^{-1} to the feature peak of S. Also was observed at 1116 cm^{-1} and 1012 cm^{-1} peaks in the spectra attributed to S–O and S–phenyl bonds of sulfonic acid. Peaks of C,

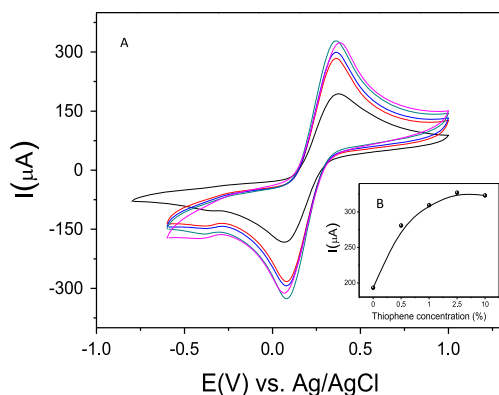


Fig. 4. Effect of the concentration of the thiophene monomer in the presence of 5 mmol L^{-1} of $\text{K}_3\text{Fe}(\text{CN})_6/\text{K}_4\text{Fe}(\text{CN})_6$, at a scanning rate of 50 mV s^{-1} .

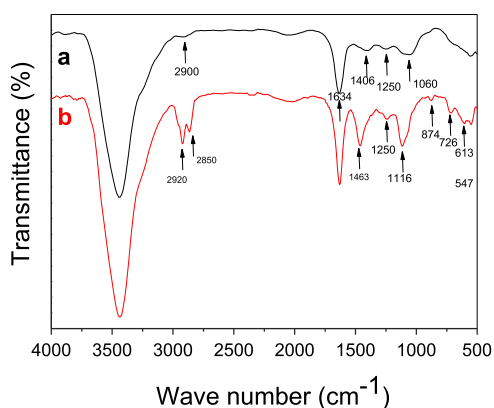


Fig. 5. ATR-FTIR spectra of the SPE—(a) without thiophene; and (b) with thiophene.

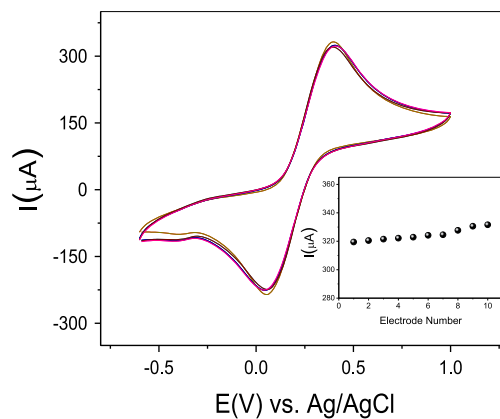


Fig. 6. Study of the reproducibility and stability of printed electrodes modified with thiophene. Ten screen-printed electrodes were tested in the presence of 5 mmol L^{-1} of $\text{K}_3\text{Fe}(\text{CN})_6/\text{K}_4\text{Fe}(\text{CN})_6$ at a scanning rate of 50 mV s^{-1} .

C–C, and C–S bonds in the thiophene backbone at 1463 cm^{-1} , 874 cm^{-1} , and 726 cm^{-1} , respectively, was also indicated [24]. Focusing on the 1450 cm^{-1} to 1370 cm^{-1} range, the band at 1434 cm^{-1} is observed together with three other weak bands at 1418 cm^{-1} , 1408 cm^{-1} , and 1400 cm^{-1} , that are typically indicative of the thiophene in the carbon ink.

3.4. Reproducibility and stability of the thiophene-SPE

SPE not only answers the criterion of cost effectiveness, but also it satisfy the previously much sought after criteria of being highly reproducible and offering sensitive methods of detection towards target analytes, whilst maintaining low cost production through scales of economy. The adaptability of SPE is also of great benefit, due to mainly its ability to easily modify the electrode through different inks or chemical compounds allows for highly specific and finely calibrated electrode to be produced for specific target analytes [25,26]. To evaluate the reproducibility of the SPE, a series of electrodes were prepared (Fig. 6a). The relative standard deviation (RSD) of the measurements for the ten electrodes was 1.28%, suggesting an acceptable precision and reproducibility. These good results should be attributed to the use of ink with a thiophene (Fig. 6). The electrodes from one series not only have the same sensitivities, but also nearly the same standard potentials, which is especially important in the case of disposable sensors.

3.5. Scan rate study

Information involving the electrochemical mechanisms can often be obtained by the relationship between the cathodic/anodic current peak and scanning rate of CV [27]. Fig. 7 shows the CVs of thiophene-SPEs at different scanning rates ranging from 10 mV s^{-1} to 100 mV s^{-1} , performed in 5 mmol L^{-1} of $\text{K}_3\text{Fe}(\text{CN})_6/\text{K}_4\text{Fe}(\text{CN})_6$ prepared in 0.1 mol L^{-1} of KCl solution, with potential ranging from -0.6 V to 1.0 V .

According to Fig. 7b, by increasing the scanning rates from 10 mV s^{-1} to 100 mV s^{-1} , the CVs of all redox couples showed a pair of symmetric peaks with a gradually increasing peak current. The currents of both the anodic and cathodic peaks increased linearly with the square root of the scanning rate, thus indicating that the process is controlled by diffusion. There was proportionality between the cathodic peak currents and the square root of the scanning rate, which shows that the charge transfer occurred reversibly. The electron transfer rate constant (k_s) was calculated employing the Laviron equation [28]:

$$k_s = \alpha n F v / RT;$$

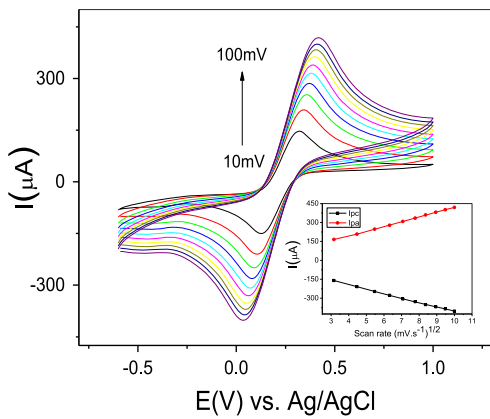


Fig. 7. (a) Cyclic voltammograms of the immunosensor in 5 mmol L⁻¹ of K₃Fe(CN)₆/K₄Fe(CN)₆ at scanning rates (from inner to outer) of: 10 mV s⁻¹, 20 mV s⁻¹, 30 mV s⁻¹, 40 mV s⁻¹, 50 mV s⁻¹, 60 mV s⁻¹, 70 mV s⁻¹, 80 mV s⁻¹, 90 mV s⁻¹, and 100 mV s⁻¹; (b) Plots of current peak as a function of the square root of the scanning rate.

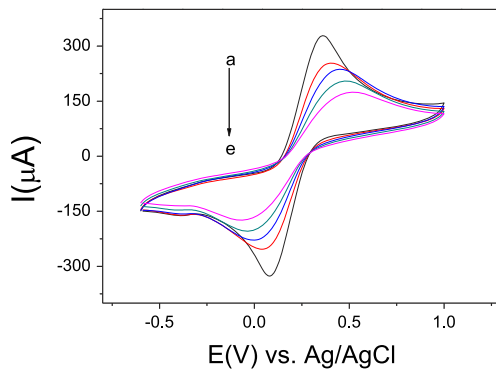


Fig. 8. Cyclic voltammograms of the immunosensor in each step of immobilization: (a) bare thiophene-SPE; (b) AuNP-Ptn-A/thiophene-SPE; (c) anti-NS1/AuNP-Ptn-A/thiophene-SPE; (d) glycine/anti-NS1/AuNP-Ptn-A/thiophene-SPE and (e) NS1/glycine/anti-NS1/AuNP-Ptn-A/thiophene-SPE. Scans were performed in 5 mmol L⁻¹ of K₃Fe(CN)₆/K₄Fe(CN)₆, at a scanning rate of 0.1 V s⁻¹.

where α is the electron transfer coefficient, n is the number of electrons transferred, F is the Faraday constant, ν is the scanning rate, R is the gas constant and T is the temperature. The ks was estimated to be $1.2 \times 10^4 \text{ s}^{-1}$.

3.6. Immobilization of the anti-NS1

CV is a very versatile electrochemical technique which allows probing of the mechanics of redox reactions and transport properties of a system in solution. When well defined redox mediators are used, CV can be utilized to characterize the stepwise modifications of the occurred at the interface of electrode surface by changes on conductivity/reactivity properties. As shown at Fig. 8, when the thiophene-SPE was coated with gold-conjugated protein A film, a decrease of the anodic and cathodic peaks was observed. Although the presence of AuNP on the electrode surface increase the electroactive area, producing a nanostructured regions, the insulating nature of protein A is probably responsible by hindering the electronic transfer [19]. According to the area of the redox peaks, a decrease of electroactive area at approximately 23% was observed. Also was observed a decrease of redox peaks after anti-NS1 antibodies immobilization and glycine blocking as expected [16].

The role of nanogold layer onto the thiophene-modified screen printed electrode was not only to increase the amount of immobilized anti-NS1 antibodies [6], but also promote an oriented immobilization of antibodies by their Fc terminal. Therefore, this

simple strategy improves the sensitivity and selectivity of the immunosensor [29,30].

3.7. Analytical response of the immunosensor

Under optimized experimental conditions, the calibration curve of the immunosensor was obtained. The electrodes were incubated in different concentrations of NS1 and submitted to CV measurements in presence of K₃[Fe(CN)₆]/K₄[Fe(CN)₆] (5 mmol L⁻¹) in KCl (0.1 mmol L⁻¹). The results show that the anodic peak current decreased with the increase of NS1 concentration in the incubation solution (Fig. 9a). Linearity in the calibration curve was obtained over

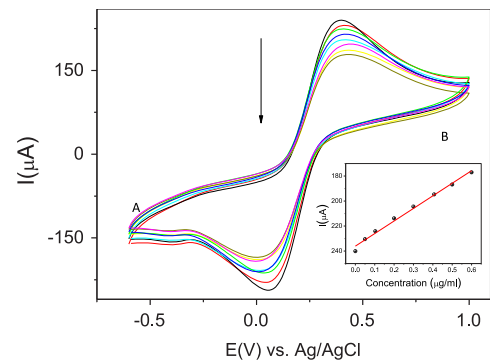


Fig. 9. (a) Cyclic voltammograms of the immunosensor in different NS1 concentrations (b) Calibration curve obtained by the anodic peaks from three replicated measurements.

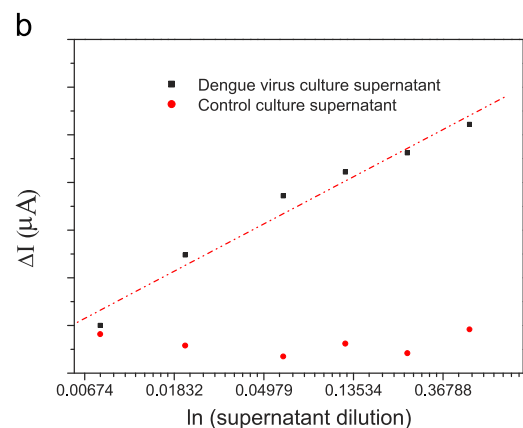
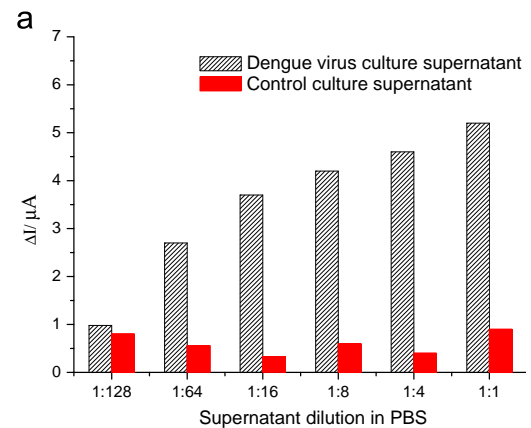


Fig. 10. (a) Analytical responses of thiophene-SPEs to the NS1 native protein f from dengue virus and control (CD4 cells) culture supernatant at serial dilutions. (b) Linear fit obtained by natural logarithm of supernatants dilutions. The amperometric responses obtained by DDP in 5 mmol L⁻¹ of K₃Fe(CN)₆/K₄Fe(CN)₆.

the range of 0.05 g mL^{-1} to 0.6 g mL^{-1} of NS1 ($r=0.991$). The limit of detection (LOD) defined as three times the blank standard deviation signal was found to be $0.015 \mu\text{g mL}^{-1}$, which was much lower than the other methods used to detect the NS1 antigen [16,31,32]. Alcon et al. [7] reported that the NS1 antigen was found circulating from the first day after onset of the illness up until the 9th day. In primary infections, NS1 levels range from $0.05 \mu\text{g mL}^{-1}$ to $0.6 \mu\text{g mL}^{-1}$ in serum samples of patients in the acute phase of the disease (up to 7 days). These clinical range for dengue diagnostic are matched with values detected by the gold nanoparticle thiophene-SPE developed.

3.8. Determination of NS1 in real samples

The proposed immunosensor was tested against real NS1 samples through culture supernatant collected on the 5th day after inoculation in C6/36 cell monolayers, period which the NS1 native protein reach maximal production [7]. The immunoelectrodes were incubated with $10 \mu\text{L}$ of a serial two-fold dilution of dengue virus culture supernatants in PBS for 30 min, at room temperature and specific responses were obtained regarding control supernatant (C6/36 cell culture). Immunosensor responses for all serial dilutions of the control culture (1:128, 1:64, 1:32, 1:16, 1:8, 1:4 to 1:1) were practically constant and similar to 1:128 dilution of control culture supernatants, whereas dengue virus supernatant responses increased inversely proportional to serial dilutions (Fig. 10a). Linear fit obtained by natural logarithm from curve shown in Fig. 9A, shows a correlation coefficient of 0.996 ($n=6$, $p < 0.01$) that is indicative of a good linearity (Fig. 10b). This label-free immunosensor is more practical than ELISA and also provide quantitative responses contrary to RDTs [33].

4. Conclusions

Thiophene monomers incorporated into the carbon ink resulted in more stable, sensible and reproducible screen printed electrodes. Moreover, nanolayer formed by gold conjugated to protein A resulted more antibodies immobilized on the electrode surface and non-random linkage. this encouraging results indicate that this chemically-modified carbon-based can be used to specific NS1 detection. Moreover, this developed immunosensor can easily become a point-of-care testing for early diagnostic of acute-phase.

Acknowledgements

The authors thank the National Council of Scientific and Technological Development (CNPq, Brazil) and the Pernambuco Research Foundation (FACEPE, PE, Brazil) for financial support.

References

- [1] J.L. Kyle, E. Harris, *Annu. Rev. Microbiol.* 62 (2008) 71–92.
- [2] A.T.A. Mairuhu, J. Wagenaar, D.P.M. Brandjes, E.C.M. van Gorp, *Eur. J. Clin. Microbiol. Infect. Dis.* (2004) 425–433.
- [3] S.D. Blacksell, R.G. Jarman, R.V. Gibbons, A. Tanganuchitcharncha, M. P. Mammen, A. Nisalak, S. Kalayanarooj, M.S. Bailey, R. Premaratna, H.J. de Silva, N.P.J. Day, D.G. Lalloo, *Clin. Vaccine Immunol.* 19 (2012) 804–810.
- [4] WHO, Special Programme for Research, Training in Tropical Diseases, Dengue: guidelines for diagnosis, treatment, prevention and control, World Health, 2009.
- [5] M.L. Moi, T. Omatsu, S. Tajima, C.-K. Lim, A. Kotaki, M. Ikeda, F. Harada, M. Ito, M. Saijo, I. Kurane, T. Takasaki, *J. Travel Med.* 20 (2013) 185–193.
- [6] S.D. Blacksell, *J. Biomed. Biotechnol.* (2012) 1–12 (Article ID 151967).
- [7] S. Alcon, A. Talarmin, M. Debruyne, A. Falconar, V. Deubel, M. Flamand, *J. Clin. Microbiol.* 40 (2002) 376–381.
- [8] S.R. Fry, M. Meyer, M.G. Semple, C.P. Simmons, S.D. Sekaran, J.X. Huang, C. McElnea, C.-Y. Huang, A. Valks, P.R. Young, M.A. Cooper, *PLoS Negl. Trop. Dis.* 5 (2011) e1199.
- [9] G.-J. Zhang, L. Zhang, M.J. Huang, Z.H.H. Luo, G.K.I. Tay, E.-J.A. Lim, T.G. Kang, Y. Chen, *Sens. Actuators, B* 146 (2010) 138–144.
- [10] T.Q. Huy, N.T.H. Hanh, N.T. Thuy, P. Van Chung, P.T. Nga, M.A. Tuan, *Talanta* 86 (2011) 271–277.
- [11] S.D. Blacksell, R.G. Jarman, M.S. Bailey, A. Tanganuchitcharnchai, K. Jenjaroen, R.V. Gibbons, D.H. Paris, R. Premaratna, H.J. de Silva, D.G. Lalloo, N.P.J. Day, *Clin. Vaccine Immunol.* 18 (2011) 2095–2101.
- [12] F. Ricci, G. Adornetto, G. Palleschi, *Electrochim. Acta* 84 (2012) 74–83.
- [13] V. Somers, J. Leaner, R. Mason, E. Iwuoha, A. Morrin, *Electrochim. Acta* 55 (2010) 4240–4246.
- [14] A.C.M.S. Dias, S.L.R. Gomes-Filho, M.M.S. Silva, R.F. Dutra, *Biosens. Bioelectron.* 44 (2013) 216–221.
- [15] O.D. Renedo, M.A. Alonso-Lomillo, M.J.A. Martínez, *Talanta* 73 (2007) 202–219.
- [16] Y. Yoshioka, G.E. Jabbour, *Synth. Met.* 156 (2006) 779–783.
- [17] J.E.N. Dolatabadi, M. Guardiabi, *Anal. Methods* 6 (2014) 3891–3900.
- [18] I.T. Cavalcanti, M.I.F. Guedes, M.D.P.T. Sotomayor, H. Yamanaka, R.F. Dutra, *Biochem. Eng. J.* 67 (2012) 225–230.
- [19] T.H. Sisson, C.W. Castor, *J. Immunol. Methods* 127 (1990) 215–220.
- [20] R.S. Lanciotti, C.H. Calisher, D.J. Gubler, G.J. Chang, A.V. Vorndam, *J. Clin. Microbiol.* 30 (1992) 545–551.
- [21] M.A. Alonso-Lomillo, O. Domínguez-Renedo, L. Ferreira-Gonçalves, M.J. Arcos-Martínez, *Biosens. Bioelectron.* 25 (2010) 1333–1337.
- [22] N.R. Stradiotto, H. Yamanaka, M.V.B. Zanoni, *J. Braz. Chem. Soc.* 14 (2003) 159–173.
- [23] J.M. O'Reilly, R.A. Mosher, *Carbon N. Y.* 21 (1981) 47–51.
- [24] Z. Wu, C. Li, Z. Wei, P. Ying, Q. Xin, *J. Phys. Chem. B* 106 (2002) 979–987.
- [25] J.P. Metters, R.O. Kadara, C.E. Banks, *Analyst* 136 (2011) 1067–1076.
- [26] R. Koncki, M. Mascini, *Anal. Chim. Acta* 351 (1997) 143–149.
- [27] S.L.R. Gomes-Filho, A.C.M.S. Dias, M.M.S. Silva, B.V.M. Silva, R.F. Dutra, *Microchem. J.* 109 (2013) 10–15.
- [28] E. Laviron, *J. Electroanal. Chem. Interfacial Electrochem.* 101 (1979) 19–28.
- [29] Z. Pei, H. Anderson, A. Myrskog, G. Dunér, B. Ingemarsson, T. Aastrup, *Anal. Biochem.* 398 (2010) 161–168.
- [30] S. Babacan, P. Pivarnik, S. Letcher, A.G. Rand, *Biosens. Bioelectron.* 15 (2000) 11–12.
- [31] S. Datta, C. Wattal, *Indian J. Med. Microbiol.* 28 (2010) 107–110.
- [32] D.H. Libraty, P.R. Young, D. Pickering, T.P. Endy, S. Kalayanarooj, S. Green, D. W. Vaughn, A. Nisalak, F.A. Ennis, A.L. Rothman, *J. Infect. Dis.* 186 (2002) 1165–1168.
- [33] V.T. Hang, N.M. Nguyet, D.T. Trung, V. Tricou, S. Yoksan, N.M. Dung, T. Van Ngoc, T.T. Hien, J. Farrar, B. Wills, C.P. Simmons, *PLoS Negl. Trop. Dis.* 3 (1) (2009) e360.